

A proposal for implementing an n -qubit controlled-rotation gate with three-level superconducting qubit systems in cavity QED

Chui-Ping Yang^{1,2}

¹*Department of Physics, Hangzhou Normal University, Hangzhou, Zhejiang 310036, China and*

²*State Key Laboratory of Precision Spectroscopy, Department of Physics, East China Normal University, Shanghai 200062, China*

We present a way for implementing an n -qubit controlled-rotation gate with three-level superconducting qubit systems in cavity QED. The two logical states of a qubit are represented by the two lowest levels of each system while a higher-energy level is used for the gate implementation. The method operates essentially by preparing a W state conditioned on the states of the control qubits, creating a single photon in the cavity mode, and then performing an arbitrary rotation on the states of the target qubit with assistance of the cavity photon. It is interesting to note that the basic operational steps for implementing the proposed gate do not increase with the number n of qubits, and the gate operation time decreases as the number of qubits increases. This proposal is quite general, which can be applied to various types of superconducting devices in a cavity or coupled to a resonator.

PACS numbers: 03.67.Lx, 42.50.Dv, 85.25.Cp

I. INTRODUCTION

Multiqubit controlled gates are of importance in constructing quantum computation circuits and quantum information processing. A multiqubit controlled gate can in principle be decomposed into the single-qubit and two-qubit gates and thus can be built based on these elementary gates. However, when using the conventional gate-decomposition protocols to construct a multiqubit controlled gate [1-3], the procedure usually becomes complicated as the number of qubits increases. This is because single-qubit and two-qubit gates, required for constructing a multiqubit controlled gate, heavily depends on the number of qubits. Therefore, finding a more efficient way to implement multiqubit controlled gates becomes important.

During the past few years, based on cavity QED technique, several theoretical proposals for implementing an n -qubit controlled-phase gate with ion traps, superconducting qubits coupled to a resonator or atoms trapped in a cavity have been presented [4-10]. These previous works opened a new way for the physical implementation of multiqubit controlled-phase (or controlled-NOT) gates, which play a significant role in quantum information processing, such as quantum algorithms [11,12] and quantum error-correction protocols [13]. On the other hand, experimental realization of a three-qubit controlled-phase gate in NMR quantum systems has been reported [14]. Moreover, a three-qubit quantum gate in trapped ions has been experimentally demonstrated recently [15].

The existing proposals in [4-10] for realizing an n -qubit controlled-phase gate can not be extended to realize an n -qubit controlled-rotation gate (denoted as controlled- R gate below). Note that multiqubit controlled- R gates are useful in quantum information processing. For instance, they can be used to construct quantum circuits for: (i) general multiqubit gates [16], (ii) preparation of arbitrary pure quantum states of multiple qubits [17], (iii) transformation of quantum states of multiple qubits [18], and (iv) quantum error correction [19]. In addition, multiqubit controlled- R gates can be applied to construct quantum circuits for implementation of quantum algorithms [20] and quantum cloning [21], and so on. In this work, we will focus on how to realize multiqubit controlled- R gates with superconducting qubit systems. As is well known, superconducting devices have appeared to be among the most promising candidates for building quantum information processors recently, due to their design flexibility, large-scale intergration, and compatibility to conventional electronics.

We note that if an n -qubit controlled- R gate is constructed by using the conventional gate-decomposition protocols, $2^n - 3$ two-qubit controlled gates would be needed (for $n \geq 3$) [1]. Thus, assuming that realizing any two-qubit controlled gate requires one-step operation only, at least $2^n - 3$ steps of operations are required, which increase with the number n of qubits *exponentially*. For instance, by using the conventional gate-decomposing protocols, 29 basic operational steps are required to implement a five-qubit controlled- R gate, and 61 basic operational steps are required to realize a six-qubit controlled- R gate.

In the following, we will propose a way for implementing an n -qubit controlled- R gate with three-level superconducting qubit systems in cavity QED. The method operates essentially based on this idea: prepare a W state conditional to the states of the control qubits, create a single photon in the cavity mode, and then perform an arbitrary rotation on the states of the target qubit with assistance of the cavity photon. The W state used for the gate implementation

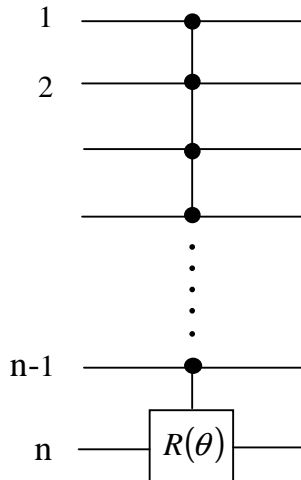


FIG. 1: Schematic circuit of an n -qubit controlled- R gate. If and only if the $n - 1$ control qubits on the filled circles (qubits $1, 2, \dots$, and $n - 1$) are all in the state $|1\rangle$, a unitary rotation $R(\theta)$ is performed on the two logical states $|0\rangle$ and $|1\rangle$ of the target qubit (qubit n), by $|0\rangle \rightarrow \cos \theta |0\rangle + \sin \theta |1\rangle$ and $|1\rangle \rightarrow -\sin \theta |0\rangle + \cos \theta |1\rangle$.

is defined as follows

$$\frac{1}{\sqrt{n-1}} \sum P_z |1\rangle^{\otimes(n-2)} |2\rangle, \quad (1)$$

where P_z is the symmetry permutation operator for qubit systems $(1, 2, \dots, n - 1)$, $\sum P_z |1\rangle^{\otimes(n-2)} |2\rangle$ denotes the totally symmetric state in which one of qubit systems $(1, 2, \dots, n - 1)$ is in the state $|2\rangle$ while the remaining $n - 2$ qubit systems are in the state $|1\rangle$. For instance, the W state is $\frac{1}{\sqrt{3}}(|112\rangle + |121\rangle + |211\rangle)$ for $n - 1 = 3$. Note that W -class entangled states were originally proposed by Dür *et al.* [22], which are useful in quantum information.

As shown below, our method only needs 7 steps of operations, which is *independent* of the number n of qubits. Thus, when compared with the gate operations required by the conventional gate-decomposition protocols, the gate operations in this proposal are greatly simplified, especially when the number n of qubits is large. Furthermore, we note that the gate operation time for this proposal decreases as the number of qubits increases. The present proposal is quite general, which can be applied to various types of superconducting devices in a cavity or coupled to a resonator.

This proposal requires adjustment of the level spacings of the qubit systems. For solid-state qubit systems such as superconducting devices, the level spacings can be rapidly adjusted (e.g., in $1 \sim 2$ nanosecond timescale for superconducting qubits [23]), by varying the external parameters (e.g., the external magnetic flux for superconducting charge qubits, the flux bias or current bias in the case of superconducting phase qubits and flux qubits, see e.g. [24-28]). It should be mentioned that tuning the level spacings to have individual qubit systems coupled to or decoupled from the cavity mode was earlier proposed for the physical realization of quantum information processing with superconducting devices (e.g., see [5,29-31]).

This paper is organized as follows. In Sec. II, we introduce the n -qubit controlled- R gate studied in this work. In Sec. III, we discuss how to prepare the W state conditioned on the states of the control qubits in cavity QED. In Sec. IV, we present a way for implementing the n -qubit controlled- R gate with three-level superconducting qubit systems in a cavity. In Sec. V, we give a brief discussion of the experimental feasibility for implementing a six-qubit controlled-Hadamard gate with superconducting devices coupled to a resonator. A concluding summary is provided in Sec. VI.

II. N -QUBIT CONTROLLED- R GATE

For n qubits, there are a total number of 2^n computational basis states, which form a set of complete orthogonal bases in a 2^n -dimensional Hilbert space of the n qubits. A quantum controlled- R gate of n qubits considered in this paper is defined by the following transformation:

$$|i_1 i_2 \cdots i_{n-1}\rangle |i_n\rangle \rightarrow \begin{cases} |i_1 i_2 \cdots i_{n-1}\rangle R(\theta) |i_n\rangle, & \text{if } \prod_{k=1}^{n-1} i_k = 1 \\ |i_1 i_2 \cdots i_{n-1}\rangle |i_n\rangle, & \text{if } \prod_{k=1}^{n-1} i_k = 0 \end{cases} \quad (2)$$

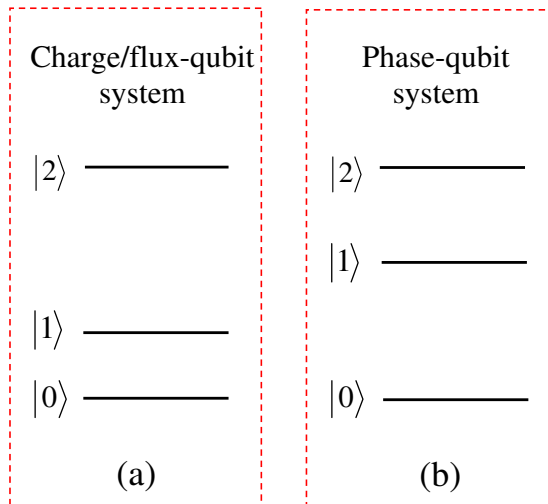


FIG. 2: (Color online) Illustration of three-level superconducting qubit systems. In (a), the level spacing between the two upper levels is larger than that between the two lower levels. In (b), vice versa.

for all $i_1, i_2, \dots, i_n \in \{0, 1\}$. Here, the subscripts 1, 2, ..., and $n - 1$ represent the $n - 1$ control qubits (1, 2, ..., $n - 1$) while the subscript n represents the target qubit n ; and $|i_1 i_2 \dots i_{n-1}\rangle |i_n\rangle$ is the n -qubit computational basis state. The operator $R(\theta)$ is described by the following matrix

$$R(\theta) = \begin{pmatrix} \cos \theta & -\sin \theta \\ \sin \theta & \cos \theta \end{pmatrix} \quad (3)$$

in a single-qubit computational subspace formed by the two logic states $|0\rangle = (1, 0)^T$ and $|1\rangle = (0, 1)^T$ of the target qubit n . It can be seen from Eq. (2) that if and only if the $n - 1$ control qubits (1, 2, ..., $n - 1$) are all in the state $|1\rangle$, a unitary rotation $R(\theta)$ is performed on the two logic states $|0\rangle$ and $|1\rangle$ of the target qubit n . The definition of the n -qubit controlled- R gate here is also shown in Fig. 1.

III. PREPARATION OF THE W STATE CONDITIONED ON THE STATES OF THE CONTROLS

In this section, we will discuss how to prepare the W state given in Eq. (1), when the $n - 1$ control qubits are initially in a computational basis state $|11\dots 1\rangle$. For the gate purpose, the remaining $2^{n-1} - 1$ computational states of the $n - 1$ control qubits need to be not affected during the W state preparation. In this section, we will also give a discussion on how this can be achieved.

The superconducting qubit systems have the three levels shown in Fig. 2. Note that the three-level structure in Fig. 2(a) applies to superconducting charge-qubit or flux-qubit systems [24,25] and the one in Fig. 2(b) applies to phase-qubit systems [26,27]. In addition, the three-level structure in Fig. 2(b) is also available in atoms. In Fig. 2, the transition between the two lowest levels $|0\rangle$ and $|1\rangle$ is assumed to: (i) be forbidden due to the selection rules, (ii) very weak due to the potential barrier between the two lowest levels, or (iii) highly detuned (decoupled) from the cavity mode during the gate operation. Throughout this paper, the two logic states of a qubit are represented by the two lowest levels $|0\rangle$ and $|1\rangle$.

To simplify our presentation, we will restrict our discussion to the three-level structure in Fig. 2(a). However, it should be mentioned that the results presented in this section and the method proposed in next section for the gate implementation are applicable to the quantum systems with the three-level structure depicted in Fig. 2(b).

Consider $n - 1$ three-level superconducting qubit systems (1, 2, ..., $n - 1$) in a single-mode cavity. The $n - 1$ systems play the role of controls in realization of the n -qubit controlled- R gate, discussed in next section. Assume that the cavity mode is coupled to the $|1\rangle \leftrightarrow |2\rangle$ transition but does not affect the level $|0\rangle$ (Fig. 3), which can be achieved by prior adjustment of the level spacings [24-28]. The Hamiltonian is given by (assuming $\hbar = 1$)

$$H = \omega_0 S_z + \omega_c a^\dagger a + g (a^\dagger S^- + a S^+), \quad (4)$$

where $S_z = \frac{1}{2} \sum_{j=1}^{n-1} (|2\rangle_j \langle 2| - |1\rangle_j \langle 1|)$, $S^+ = \sum_{j=1}^{n-1} |2\rangle_j \langle 1|$, $S^- = \sum_{j=1}^{n-1} |1\rangle_j \langle 2|$, a^\dagger and a are the photon creation and annihilation operators for the cavity mode, ω_c is the cavity-mode frequency, ω_0 is the $|1\rangle \leftrightarrow |2\rangle$ transition frequency, and g is the coupling constant between the cavity mode and the $|1\rangle \leftrightarrow |2\rangle$ transition.

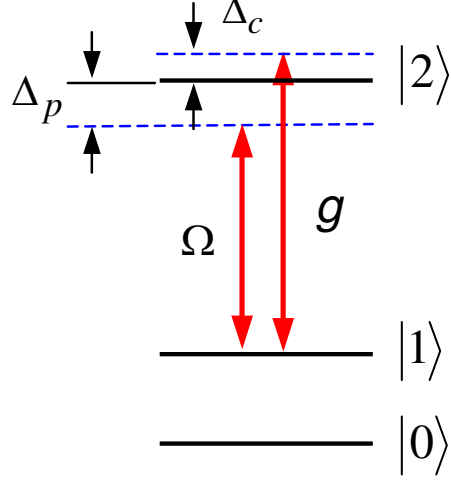


FIG. 3: (Color online) The transition between the two lowest levels is forbidden due to the selection rules, very weak due to the potential barrier between the two lowest levels, or highly detuned (decoupled) from the cavity mode. The $|1\rangle \leftrightarrow |2\rangle$ transition is non-resonantly coupled to the cavity mode with a detuning Δ_c , and non-resonantly coupled to the classical pulse with a detuning Δ_p .

In the case when the detuning $\Delta_c = \omega_c - \omega_0 \gg g\sqrt{\bar{n} + 1}$ with \bar{n} being the mean photon number of the cavity mode, the Hamiltonian (4) can be rewritten as follows [32]

$$H = \omega_0 S_z + \omega_c a^\dagger a - \lambda \left[\sum_{j=1}^{n-1} (|2\rangle_j \langle 2| - |1\rangle_j \langle 1|) a^\dagger a \right] - \lambda S^+ S^-, \quad (5)$$

where $\lambda = g^2/\Delta_c$. The third term describes the photon-number dependent Stark shift while the last term describes the dipole coupling among the $n-1$ qubit systems. If the cavity mode is initially in the vacuum state $|0\rangle$, the Hamiltonian (5) reduces to

$$H_0 = \omega_0 S_z - \lambda S^+ S^-. \quad (6)$$

If the $n-1$ control qubits are initially in the computational basis state $|11\dots 1\rangle$, i.e., the Dicke state $|J, -J\rangle$ with $J = (n-1)/2$, they evolve within the symmetric Dicke subspace spanned by $\{|J, -J\rangle, |J, -J+1\rangle, \dots, |J, J\rangle\}$. Here, the state $|J, -J+k\rangle$ with $k = 0, 1, \dots, n-1$ is a symmetric Dicke state with k systems being in the state $|2\rangle$ while $n-k-1$ systems being in the state $|1\rangle$. The Dicke state $|J, -J+k\rangle$ is given by

$$|J, -J+k\rangle = \frac{1}{\sqrt{\binom{n-1}{k}}} \sum P_z |1\rangle^{\otimes(n-k-1)} |2\rangle^{\otimes k}, \quad (7)$$

where P_z is the symmetry permutation operator for systems $(1, 2, \dots, n-1)$, $\sum P_z |1\rangle^{\otimes(n-k-1)} |2\rangle^{\otimes k}$ denotes the totally symmetric state in which $n-k-1$ of systems $(1, 2, \dots, n-1)$ are in the state $|1\rangle$ while the remaining k systems are in the state $|2\rangle$.

One can check that the Hamiltonian H_0 has the following properties

$$H_0 |J, -J+k\rangle = \varepsilon_k |J, -J+k\rangle, \quad (8)$$

with

$$\varepsilon_k = \omega_0 (-J+k) - k(2J-k+1)\lambda. \quad (9)$$

Eq. (8) demonstrates that the Dicke state $|J, -J+k\rangle$ is the eigenstate of the Hamiltonian H_0 with the eigenvalue ε_k . The energy-level spacing between $|J, -J+k\rangle$ and $|J, -J+k+1\rangle$ is $\varepsilon_{k+1} - \varepsilon_k = \omega_0 - 2(J-k)\lambda$, depending on

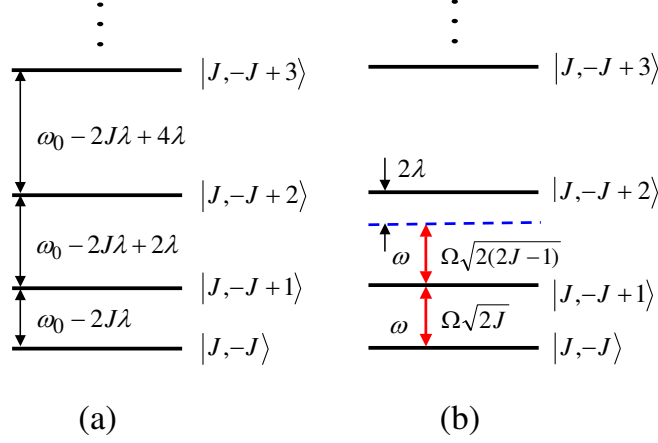


FIG. 4: (Color online) (a) Non-identical level spacings for the energy levels. The level spacings between two adjacent levels become wider by 2λ as the energy levels go up. (b) Illustration of the pulse (with frequency $\omega = \omega_0 - 2J\lambda$) resonantly coupled to the transition between the two lowest Dicke states $|J, -J\rangle$ and $|J, -J+1\rangle$ but detuned from the $|J, -J+1\rangle \leftrightarrow |J, -J+2\rangle$ transition with a detuning 2λ .

the excitation number of the state $|J, -J+k\rangle$. It can be seen that the energy level spacings in the symmetric Dicke subspace are unequal [Fig. 4(a)]. For the detailed discussion, see Ref. [33].

To prepare the W state of Eq. (1), we now apply an external driving pulse (with frequency ω) to the $n-1$ systems $(1, 2, \dots, n-1)$. Suppose that the pulse is coupled to the $|1\rangle \leftrightarrow |2\rangle$ transition but far-off resonant with the transition between any other two levels of each system (Fig. 3). Thus, the interaction Hamiltonian between the pulse and the $n-1$ systems is given by

$$H_{sp} = \Omega (e^{-i\omega t} S^+ + e^{i\omega t} S^-), \quad (10)$$

where Ω is the Rabi frequency of the pulse. The Hamiltonian for the whole system is

$$\tilde{H} = H_0 + H_{sp} \quad (11)$$

Performing the transformation $U = e^{i\omega t S_z}$, we obtain the engineered Hamiltonian in the symmetric Dicke subspace

$$\begin{aligned} H' &= U \tilde{H} U^\dagger - \omega S_z \\ &= \sum_{k=0}^{n-1} \delta_k |J, -J+k\rangle \langle J, -J+k| \\ &\quad + \sum_{k=0}^{n-2} \Omega_k (|J, -J+k+1\rangle \langle J, -J+k| + \text{H.c.}), \end{aligned} \quad (12)$$

where

$$\begin{aligned} \Omega_k &= \Omega \sqrt{(2J-k)(k+1)}, \\ \delta_k &= \omega_0(-J+k) - k(2J-k+1)\lambda - \omega(-J+k). \end{aligned} \quad (13)$$

Assume that the applied pulse is resonant with the transition between the Dicke states $|J, -J\rangle$ and $|J, -J+1\rangle$ [Fig. 4(b)]. Namely, the pulse frequency ω is set by $\omega = \omega_0 - 2J\lambda$, i.e., $\Delta_p = \omega_0 - \omega = 2J\lambda$ (Fig. 3). Discarding the constant energy $-2J^2\lambda$ we have $\delta_0 = \delta_1 = 0$ and $\delta_k = k(k-1)\lambda$ ($k \geq 2$). Hence the detuning of the pulse frequency with the transition frequency between the two energy levels $|J, -J+1\rangle$ and $|J, -J+2\rangle$ is 2λ [Fig. 4(b)]. Therefore, if we have $\Omega\sqrt{2(2J-1)} \ll 2\lambda$, which is guaranteed by setting

$$\Omega\sqrt{n-1} \ll \lambda, \quad (14)$$

then the transition between the two Dicke states $|J, -J + 1\rangle$ and $|J, -J + 2\rangle$ is negligible due to far-off resonance with the pulse. As a result, when the systems $(1, 2, \dots, n - 1)$ are initially in the Dicke state $|J, -J\rangle$ or $|J, -J + 1\rangle$, the Dicke state $|J, -J + 2\rangle$ will not be excited by the pulse and therefore no transition from the state $|J, -J + 2\rangle$ to any one of the Dicke states $\{|J, -J + 3\rangle, |J, -J + 4\rangle, \dots, |J, J\rangle\}$ occurs. The Hamiltonian H' thus reduces to

$$H' = \Omega\sqrt{2J}(|J, -J + 1\rangle \langle J, -J| + \text{H.c.}). \quad (15)$$

It is straightforward to show from Eq. (15) that the states $|J, -J\rangle$ and $|J, -J + 1\rangle$ evolve as follows

$$|J, -J\rangle \rightarrow \cos(\sqrt{2J}\Omega t)|J, -J\rangle - i\sin(\sqrt{2J}\Omega t)|J, -J + 1\rangle, \quad (16)$$

$$|J, -J + 1\rangle \rightarrow \cos(\sqrt{2J}\Omega t)|J, -J + 1\rangle - i\sin(\sqrt{2J}\Omega t)|J, -J\rangle. \quad (17)$$

Based on Eq. (1) and Eq. (7), it can be seen that the Dicke state $|J, -J + 1\rangle$ here is the W state defined in Eq. (1).

From Eq. (16), it can be seen that when the control qubits $(1, 2, \dots, n - 1)$ are initially in the state $|J, -J\rangle$ (i.e., the computational state $|11\dots 1\rangle$), the W state $|J, -J + 1\rangle$ is prepared through a transformation $|J, -J\rangle \rightarrow -i|J, -J + 1\rangle$ after a pulse duration $t = \pi/(2\sqrt{2J}\Omega)$.

For the gate implementation below, we will need to transform the prepared W state $|J, -J + 1\rangle$ back to the state $|J, -J\rangle$. Eq. (17) shows that this can be achieved by applying the same pulse to the systems $(1, 2, \dots, n - 1)$ for a time $t = \pi/(2\sqrt{2J}\Omega)$, via the transformation $|J, -J + 1\rangle \rightarrow -i|J, -J\rangle$.

The remaining $(2^{n-1} - 1)$ computational basis states $|i_1 i_2 \dots i_{n-1}\rangle$ of the $n - 1$ control qubit systems can be classified into a set of Dicke states $\{|J - l/2, -(J - l/2)\rangle\}$ with $l = 1, 2, \dots, n - 1$. For instance, the $(n - 1)$ -qubit computational basis states $|11\dots 110\rangle$ and $|11\dots 100\rangle$ can be written in term of the Dicke states $|J - 1/2, -(J - 1/2)\rangle$ (for $l = 1$) and $|J - 1, -(J - 1)\rangle$ (for $l = 2$), respectively. To see how the set of Dicke states $\{|J - l/2, -(J - l/2)\rangle\}$ here not to be affected during the W state preparation, let us focus on a Dicke state $|J - l/2, -(J - l/2)\rangle$ ($l \neq 0$), and discuss how to make this Dicke state unaffected by the pulse.

The level spacing between the Dicke states $|J - l/2, -(J - l/2)\rangle$ and $|J - l/2, -(J - l/2) + 1\rangle$ is given by

$$\tilde{\epsilon}_1 - \tilde{\epsilon}_0 = \omega_0 - (2J - l)\lambda. \quad (18)$$

Therefore, the detuning of the pulse frequency from the transition frequency between the two Dicke states $|J - l/2, -(J - l/2)\rangle$ and $|J - l/2, -(J - l/2) + 1\rangle$ would be $\omega - (\tilde{\epsilon}_1 - \tilde{\epsilon}_0) = -l\lambda$. The pulse Rabi frequency between the two Dicke states $|J - l/2, -(J - l/2)\rangle$ and $|J - l/2, -(J - l/2) + 1\rangle$ is $\Omega\sqrt{2J - l}$, which can be seen from the expression of Ω_k in Eq. (13) (for the present case, $k = 0$ and J is replaced by $J - l/2$). If the large detuning $\Omega\sqrt{2J - l} \ll l\lambda$ is met, the transition between the two Dicke states $|J - l/2, -(J - l/2)\rangle$ and $|J - l/2, -(J - l/2) + 1\rangle$ can be neglected due to far-off resonance with the pulse. Thus, the pulse does not excite the Dicke state $|J - l/2, -(J - l/2) + 1\rangle$ when the control qubits $(1, 2, \dots, n - 1)$ are initially in the state $|J - l/2, -(J - l/2)\rangle$.

Note that for any $l \in \{1, 2, \dots, n - 1\}$, we have $\Omega\sqrt{2J - l} \ll l\lambda$ when $\Omega\sqrt{n - 1} \ll \lambda$. Therefore, as long as the condition in Eq. (14) is satisfied, the Dicke state $|J - l/2, -(J - l/2)\rangle$ with any given $l = 1, 2, \dots, n - 1$ will not be affected by the pulse, i.e., the rest $(2^{n-1} - 1)$ computational basis states of the control qubit systems $(1, 2, \dots, n - 1)$ remain unchanged during the pulse.

IV. IMPLEMENTATION OF AN N -QUBIT CONTROLLED- R GATE IN CAVITY QED

Let us now consider n superconducting qubit systems $(1, 2, \dots, n)$ placed in a cavity or coupled to a resonator. Each system has the three-level configuration. Initially, the transition between any two levels of each system is highly detuned (decoupled) from the cavity mode [Fig. 5(a, a')], which can be achieved via prior adjustment of the level spacings. In addition, assume that the cavity mode is initially in the vacuum state $|0\rangle_c$.

The procedure for implementing the n -qubit controlled- R gate is listed as follows:

Step (i): Leave the level structure of system n unchanged [Fig. 5(b')] while adjusting the level spacings of systems $(1, 2, \dots, n - 1)$ such that the $|1\rangle \leftrightarrow |2\rangle$ transition of each of systems $(1, 2, \dots, n - 1)$ is non-resonantly coupled to the cavity mode, with a detuning Δ_c [Fig. 5(b)]. Then, apply a pulse to systems $(1, 2, \dots, n - 1)$ for a duration $t_1 = \pi/(2\sqrt{2J}\Omega)$ [Fig. 5(b)]. As discussed in Sec. III, when the systems $(1, 2, \dots, n - 1)$ are initially in the computational basis state $|11\dots 1\rangle$, the W state $|J, -J + 1\rangle$ is created after the pulse, via a transformation $|J, -J\rangle \rightarrow -i|J, -J + 1\rangle$. Note that the cavity mode remains in the vacuum state during the operation of this step, as shown in Sec. III.

Step (ii): Leave the level structure of system n unchanged [Fig. 5(c')] while adjusting the level spacings of systems $(1, 2, \dots, n - 1)$ such that the $|1\rangle \leftrightarrow |2\rangle$ transition of each of systems $(1, 2, \dots, n - 1)$ is resonantly coupled to the cavity

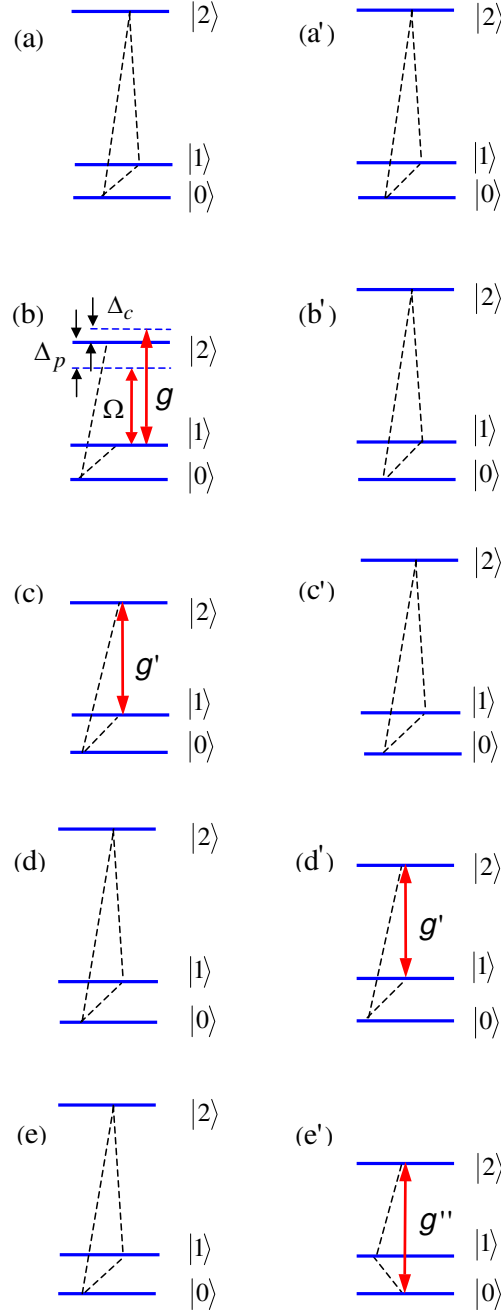


FIG. 5: (Color online) The level structures of the systems $(1, 2, \dots, n)$ during the gate preparation. Figures on the left side represent the level structures for systems $(1, 2, \dots, n-1)$, while figures on the right side represent the level structures of system n . Here, g is the non-resonantly-coupling constant between the cavity mode and the $|1\rangle \leftrightarrow |2\rangle$ transition, g' is the resonantly-coupling constant between the cavity mode and the $|1\rangle \leftrightarrow |2\rangle$ transition, and g'' is the resonantly-coupling constant between the cavity mode and the $|0\rangle \leftrightarrow |2\rangle$ transition. In addition, the transition between any two levels linked by a dashed line is highly detuned (decoupled) from the cavity mode and/or the pulse.

mode for an interaction time $t_2 = (\pi/2)/(\sqrt{2J}g')$ [Fig. 5(c)]. The Hamiltonian describing this step is given by (in the interaction picture)

$$H_I = g' a S^+ + g' a^+ S^-. \quad (19)$$

Here and below, g' is the resonantly-coupling constant between the cavity mode and the $|1\rangle \leftrightarrow |2\rangle$ transition. It can be found that under this Hamiltonian, the time evolution for the state $|J, -J+1\rangle \otimes |0\rangle_c$ of the systems $(1, 2, \dots, n-1)$

and the cavity mode is described by

$$|J, -J + 1\rangle \otimes |0\rangle_c \rightarrow \cos(\sqrt{2J}g't) |J, -J + 1\rangle \otimes |0\rangle_c - i \sin(\sqrt{2J}g't) |J, -J\rangle \otimes |1\rangle_c, \quad (20)$$

which shows that when systems $(1, 2, \dots, n-1)$ are initially in the W state $|J, -J + 1\rangle$, a single photon is created in the cavity mode after an interaction time t_2 given above, through a transformation $|J, -J + 1\rangle \otimes |0\rangle_c \rightarrow -i |J, -J\rangle \otimes |1\rangle_c$. Note that the operation time t_2 ($\propto 1/\sqrt{n-1}$) decreases as the number $n-1$ of the qubit systems increases.

Step (iii): Adjust the level spacings of systems $(1, 2, \dots, n-1)$ back to the original situation [Fig. 5(d)] such that the cavity mode does not couple to the systems $(1, 2, \dots, n-1)$. Meanwhile, adjust the level spacings of system n so that the $|1\rangle \leftrightarrow |2\rangle$ transition of this system is resonantly coupled to the cavity mode for an interaction time t_3 [Fig. 5(d')]. The Hamiltonian describing this step of operation is given by

$$H_I = \hbar (g'a^+ |1\rangle \langle 2| + \text{h.c.}). \quad (21)$$

The time evolution of the state $|1\rangle_n |1\rangle_c$ is described by

$$|1\rangle_n |1\rangle_c \rightarrow \cos(g't) |1\rangle_n |1\rangle_c - i \sin(g't) |2\rangle_n |0\rangle_c. \quad (22)$$

It can be seen from Eq. (22) that after an interaction time $t_3 = \pi/(2g')$, the state $|1\rangle_n |1\rangle_c$ changes to $-i |2\rangle_n |0\rangle_c$. Note that the state $|0\rangle_n |1\rangle_c$ remains unchanged since the state $|0\rangle_n$ is not coupled to the cavity mode. Here and below, the subscript n represents the system n .

Step (iv): Leave the level structure of systems $(1, 2, \dots, n-1)$ unchanged [Fig. 5(e)] while adjust the level spacings of system n so that the $|0\rangle \leftrightarrow |2\rangle$ transition of system n is resonantly coupled to the cavity mode for an interaction time t_4 [Fig. 5(e')]. The Hamiltonian describing this step is

$$H_I = \hbar (g''a^+ |0\rangle \langle 2| + \text{h.c.}). \quad (23)$$

Here and below, g'' is the resonantly-coupling constant between the cavity mode and the $|0\rangle \leftrightarrow |2\rangle$ transition. According to this Hamiltonian, one can easily find that after an interaction time $t_4 = \theta/g''$, the transformations $|0\rangle_n |1\rangle_c \rightarrow \cos \theta |0\rangle_n |1\rangle_c - i \sin \theta |2\rangle_n |0\rangle_c$ and $|2\rangle_n |0\rangle_c \rightarrow -i \sin \theta |0\rangle_n |1\rangle_c + \cos \theta |2\rangle_n |0\rangle_c$ are obtained.

The operations for the last three steps are the reverse operations of steps (i), (ii) and (iii) above, which are described below:

Step (v): Leave the level structure of systems $(1, 2, \dots, n-1)$ unchanged [Fig. 5(d)] while adjust the level spacings of system n such that the $|1\rangle \leftrightarrow |2\rangle$ transition of system n is resonant with the cavity mode for an interaction time t_5 [Fig. 5(d')]. The Hamiltonian describing this step is the one in Eq. (21). The time evolution of the state $|2\rangle_n |0\rangle_c$ is described by

$$|2\rangle_n |0\rangle_c \rightarrow \cos(g't) |2\rangle_n |0\rangle_c - i \sin(g't) |1\rangle_n |1\rangle_c. \quad (24)$$

Thus, after an interaction time $t_5 = 3\pi/(2g')$, the state $|2\rangle_n |0\rangle_c$ becomes $i |1\rangle_n |1\rangle_c$. Note that the state $|0\rangle_n |1\rangle_c$ remains unchanged during this step of operation.

Step (vi): Adjust the level spacings of system n such that the cavity mode does not couple to this system [Fig. 5(c')]. Meanwhile, adjust the level spacings of systems $(1, 2, \dots, n-1)$ such that the $|1\rangle \leftrightarrow |2\rangle$ transition of each of systems $(1, 2, \dots, n-1)$ is resonant with the cavity mode for an interaction time t_6 [Fig. 5(c)]. The Hamiltonian describing this step is the one in (19), from which one can easily find that the time evolution for the state $|J, -J\rangle \otimes |1\rangle_c$ of the systems $(1, 2, \dots, n-1)$ and the cavity mode is described by

$$|J, -J\rangle \otimes |1\rangle_c \rightarrow \cos(\sqrt{2J}g't) |J, -J\rangle \otimes |1\rangle_c - i \sin(\sqrt{2J}g't) |J, -J + 1\rangle \otimes |0\rangle_c. \quad (25)$$

It can be seen from Eq. (25) that the operation of this step results in the transformation $|J, -J\rangle \otimes |1\rangle_c \rightarrow -i |J, -J + 1\rangle \otimes |0\rangle_c$ for $t_6 = \pi/(2\sqrt{2J}g')$.

Step (vii): Leave the level structure of system n unchanged [Fig. 5(b')] while adjusting the level spacings of systems $(1, 2, \dots, n-1)$ such that the $|1\rangle \leftrightarrow |2\rangle$ transition of each of systems $(1, 2, \dots, n-1)$ is non-resonantly coupled to the cavity mode, with a detuning Δ_c [Fig. 5(b)]. Then, apply a pulse to systems $(1, 2, \dots, n-1)$ for a duration $t_7 = \pi/(2\sqrt{2J}\Omega)$ [Fig. 5(b)]. As discussed in Sec. III, the operation of this step leads to the transformation $|J, -J + 1\rangle \rightarrow -i |J, -J\rangle$.

Note that after the last step of operation, we will need to leave the level structure of system n unchanged [Fig. 5(a')] while adjust the level spacings of systems $(1, 2, \dots, n-1)$ back to the original situation as shown in Fig. 5(a), such that the cavity mode does not couple to each system after the above manipulation.

The states of the whole system after each step of the above operations are summarized below:

$$\begin{aligned}
& |11\dots 1\rangle |0\rangle \otimes |0\rangle_c \\
& \xrightarrow{\text{Step}^{(i)}} -i |J, -J + 1\rangle |0\rangle \otimes |0\rangle_c \\
& \xrightarrow{\text{Step}^{(ii)}} - |J, -J\rangle |0\rangle \otimes |1\rangle_c \\
& \xrightarrow{\text{Step}^{(iii)}} - |J, -J\rangle |0\rangle \otimes |1\rangle_c \\
& \xrightarrow{\text{Step}^{(iv)}} - |J, -J\rangle (\cos \theta |0\rangle |1\rangle_c - i \sin \theta |2\rangle |0\rangle_c) \\
& \xrightarrow{\text{Step}^{(v)}} - |J, -J\rangle (\cos \theta |0\rangle + \sin \theta |1\rangle) |1\rangle_c \\
& \xrightarrow{\text{Step}^{(vi)}} i |J, -J + 1\rangle (\cos \theta |0\rangle + \sin \theta |1\rangle) |0\rangle_c \\
& \xrightarrow{\text{Step}^{(vii)}} |11\dots 1\rangle (\cos \theta |0\rangle + \sin \theta |1\rangle) |0\rangle_c.
\end{aligned} \tag{26}$$

$$\begin{aligned}
& |11\dots 1\rangle |1\rangle \otimes |0\rangle_c \\
& \xrightarrow{\text{Step}^{(i)}} -i |J, -J + 1\rangle |1\rangle \otimes |0\rangle_c \\
& \xrightarrow{\text{Step}^{(ii)}} - |J, -J\rangle |1\rangle \otimes |1\rangle_c \\
& \xrightarrow{\text{Step}^{(iii)}} i |J, -J\rangle |2\rangle \otimes |0\rangle_c \\
& \xrightarrow{\text{Step}^{(iv)}} |J, -J\rangle (\sin \theta |0\rangle |1\rangle_c + i \cos \theta |2\rangle |0\rangle_c) \\
& \xrightarrow{\text{Step}^{(v)}} - |J, -J\rangle (-\sin \theta |0\rangle + \cos \theta |1\rangle) |1\rangle_c \\
& \xrightarrow{\text{Step}^{(vi)}} i |J, -J + 1\rangle (-\sin \theta |0\rangle + \cos \theta |1\rangle) |0\rangle_c \\
& \xrightarrow{\text{Step}^{(vii)}} |11\dots 1\rangle (-\sin \theta |0\rangle + \cos \theta |1\rangle) |0\rangle_c.
\end{aligned} \tag{27}$$

where $|J, -J\rangle$ (i.e., $|11\dots 1\rangle$) and $|J, -J + 1\rangle$ are the Dicke states of systems $(1, 2, \dots, n - 1)$, while $|0\rangle$, $|1\rangle$, and $|2\rangle$ are the states of system n .

On the other hand, it is noted that the following states of the whole system

$$\{|i_1 i_2 \dots i_{n-1}\rangle |0\rangle_n |0\rangle_c, |i_1 i_2 \dots i_{n-1}\rangle |1\rangle_n |0\rangle_c\} \tag{28}$$

(for all $i_1, i_2, \dots, i_{n-1} \in \{0, 1\}$ and $\prod_{k=1}^{n-1} i_k = 0$) remain unchanged during the entire operation. This is because: (a) During the operation of step (i), the states $\{|i_1 i_2 \dots i_{n-1}\rangle$ of systems $(1, 2, \dots, n - 1)$ were not affected by the applied pulse, as discussed in Sec. III; and (b) No photon was emitted to the cavity during the operation of step (ii), when systems $(1, 2, \dots, n - 1)$ are in any one of the states $\{|i_1 i_2 \dots i_{n-1}\rangle$. Hence, it can be concluded from Eqs. (26) and (27) that the transformation (2), i.e, the n -qubit controlled- R gate, was implemented with n systems (i.e., the $n - 1$ control systems $(1, 2, \dots, n - 1)$ and the target system n) after the above process.

The systems not involved in each step of the operations above need to be decoupled from the cavity field and/or the pulse. This requirement can be achieved by adjusting the level spacings (e.g., doable for superconducting devices as discussed in the introduction).

The detunings Δ_c and Δ_p are set identical for each of systems $(1, 2, \dots, n - 1)$ in steps (i) and (vii), and systems $(1, 2, \dots, n - 1)$ are brought to resonance with the cavity mode in steps (ii) and (vi). Therefore, the level spacings for systems $(1, 2, \dots, n - 1)$ can be synchronously adjusted via changing the common external parameters of the qubit systems during the entire operation. In addition, the cavity mode is virtually excited during the operation of steps (i) and (vii). Thus, decoherence caused by the cavity decay for these two steps is greatly reduced.

From the description given above, it can be seen that the level $|0\rangle$ of each of qubit systems $(1, 2, \dots, n - 1)$ is not affected during the entire operation, because the cavity mode was set to be highly detuned (decoupled) from the $|0\rangle \leftrightarrow |1\rangle$ transition and the $|0\rangle \leftrightarrow |2\rangle$ transition. Thus, the level spacing between the two levels $|0\rangle$ and $|1\rangle$ and the level spacing between the two levels $|0\rangle$ and $|2\rangle$ are both not required to be identical for each of qubit systems $(1, 2, \dots, n - 1)$. However, as shown above, the level spacing between the two levels $|1\rangle$ and $|2\rangle$ needs to be identical for each of qubit systems $(1, 2, \dots, n - 1)$. Note that for superconducting qubit systems, it is difficult to have the level spacing between *any* two levels to be the same for each qubit system, but it is easy to have the level spacing between

certain two levels (i.e., the levels $|1\rangle$ and $|2\rangle$ for the present case) to be identical by adjusting device parameters or varying external parameters [34].

Finally, it should be mentioned that nonuniform of the device parameters for qubit systems $(1, 2, \dots, n-1)$ may cause the coupling strength g or g' (i.e., the coupling strength between the cavity mode and the $|1\rangle \leftrightarrow |2\rangle$ transition) not to be the same for each of qubit systems $(1, 2, \dots, n-1)$. However, it is noted that for a superconducting qubit system, the qubit-cavity coupling strength is adjustable by varying the position of the qubit system in the cavity. Thus, by having the qubit systems $(1, 2, \dots, n-1)$ located at appropriate positions of the cavity, one can have the coupling strength g or g' to be identical for each of qubit systems $(1, 2, \dots, n-1)$.

V. POSSIBLE EXPERIMENTAL REALIZATION

In this section, we give a discussion on possible experimental implementations. For the method to work:

(a) During the operation of step (i) or step (vii), the occupation probability p_1 of the Dicke state $|J, -J+2\rangle$ due to the $|J, -J+1\rangle \leftrightarrow |J, -J+2\rangle$ transition induced by the pulse, and the occupation probability p_2 of the Dicke state $|J-l/2, -(J-l/2)+1\rangle$ due to the $|J-l/2, -(J-l/2)\rangle \leftrightarrow |J-l/2, -(J-l/2)+1\rangle$ transition induced by the pulse, given by [35]

$$\begin{aligned} p_1 &\simeq \frac{\Omega^2}{\Omega^2 + \lambda^2/[2(n-2)]}, \\ p_2 &\simeq \frac{\Omega^2}{\Omega^2 + (l\lambda)^2/[4(n-l-1)]} \\ &\leq \frac{\Omega^2}{\Omega^2 + \lambda^2/[4(n-2)]}, \end{aligned} \quad (29)$$

need to be negligibly small in order to reduce the gate error.

(b) According to the discussion in Sec. III, the following conditions need to be satisfied:

$$g \ll \Delta_c, \quad \Omega\sqrt{n-1} \ll g^2/\Delta_c, \quad \Delta_p = (n-1)g^2/\Delta_c. \quad (30)$$

Note that these conditions can in principle be achieved because: (i) the Rabi frequency Ω can be adjusted by changing the intensity of the pulse, (ii) the detuning Δ_c can be adjusted by changing the $|1\rangle \leftrightarrow |2\rangle$ transition frequency ω_0 , and (iii) the detuning Δ_p can be adjusted by varying the pulse frequency ω .

(c) The total operation time is given by

$$\tau = \pi/(\Omega\sqrt{n-1}) + \pi/(g'\sqrt{n-1}) + 2\pi/g' + \theta/g'' + 8\tau_a, \quad (31)$$

which shows that for a given $\Omega\sqrt{n-1}$, the τ decreases as the number n of qubits increases. Here, τ_a is the typical time required for adjusting the level spacings during each step. The τ should be much shorter than the energy relaxation time γ_{2r}^{-1} and dephasing time γ_{2p}^{-1} of the level $|2\rangle$, such that decoherence, caused due to spontaneous decay and dephasing process of the qubit systems, is negligible during the operation. And, the τ needs to be much shorter than the lifetime of the cavity photon, which is given by $\kappa^{-1} = Q/2\pi\nu_c$, such that the decay of the cavity photon can be neglected during the operation. Here, Q is the (loaded) quality factor of the cavity and ν_c is the cavity field frequency. To obtain these requirements, one can design the qubit systems to have sufficiently long energy relaxation time and dephasing time, such that $\tau \ll \gamma_{2r}^{-1}, \gamma_{2p}^{-1}$; and choose a high- Q cavity such that $\tau \ll \kappa^{-1}$.

For the sake of definitiveness, let us consider the experimental possibility of realizing a six-qubit controlled-Hadamard gate (i.e., the controlled- R gate for $\theta = \pi/4$), using six identical superconducting qubit systems coupled to a resonator [Fig. 6(a)]. Each qubit system could be a superconducting charge-qubit system [Fig. 6(b)], flux-qubit system [Fig. 6(c)], or flux-biased phase-qubit system [Fig. 6(d)]. As a rough estimate, assume $g/2\pi \sim 220$ MHz, which could be reached for a superconducting qubit system coupled to a one-dimensional standing-wave CPW (coplanar waveguide) transmission resonator [36]. With the choice of $g', g'' \sim g$, $\Delta_c \sim 10g$, $\Omega/2\pi \sim 1.1$ MHz (i.e., $\lambda/\Omega \sim 20$), and $\tau_a \sim 1$ ns, one has $\tau \sim 0.2$ μ s, much shorter than $\min\{\gamma_{2r}^{-1}, \gamma_{2p}^{-1}\} \sim 1$ μ s [26,37]. In addition, consider a resonator with frequency $\nu_c \sim 3$ GHz (e.g., Ref. [38]) and $Q \sim 5 \times 10^4$, we have $\kappa^{-1} \sim 2.7$ μ s, which is much longer than the operation time τ here. Note that superconducting coplanar waveguide resonators with a quality factor $Q > 10^6$ have been experimentally demonstrated [39].

For the choice of $\Delta_c \sim 10g$ and $\lambda/\Omega \sim 20$ here, we have $p_1 \sim 0.02$ and $p_2 \leq 0.04$, which can be further reduced by increasing the ratio Δ_c/g and λ/Ω . How well this gate would work needs to be further investigated for each particular experimental set-up or implementation. However, we note that this requires a rather lengthy and complex analysis, which is beyond the scope of this theoretical work.

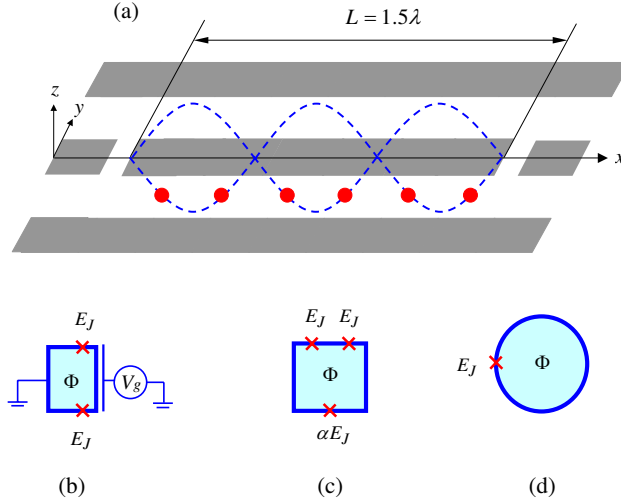


FIG. 6: (Color online) (a) Sketch of the setup for six superconducting qubit systems (red dots) and a (grey) standing-wave quasi-one-dimensional coplanar waveguide resonator. λ is the wavelength of the resonator mode, and L is the length of the resonator. The two blue curved lines represent the standing wave magnetic field, which is in the z -direction. Each qubit system (a red dot) could be a superconducting charge-qubit system shown in (b), flux-qubit system in (c), and flux-biased phase-qubit system in (d). The qubit systems are placed at locations where the magnetic fields are the same to obtain an identical coupling constant for each qubit system. The superconducting loop of each qubit system, which is a large square for (b) and (c) while a large circle for (d), is located in the plane of the resonator between the two lateral ground planes (i.e., the x - y plane). E_J is the Josephson junction energy ($0.6 < \alpha < 0.8$) and V_g is the gate voltage. In addition, the external magnetic flux Φ applied to the superconducting loop for each qubit system is created by the magnetic field threading the superconducting loop.

VI. CONCLUSION

In summary, we have proposed a way for implementing an n -qubit controlled-rotation gate with three-level superconducting qubit systems in cavity QED. This proposal requires seven steps of operation only, which is independent of the number n of qubits. In contrast, when the proposed gate is constructed by using the conventional gate-decomposing protocols, the basic operational steps increase with the number n of qubits *exponentially*. Thus, when the number n of qubits is large, the gate operation is significantly simplified by using the present proposal. In addition, as shown above, the gate operation time for this proposal decreases as the number of qubits increases. This proposal is quite general, which can be applied to various types of superconducting devices in a cavity or coupled to a resonator.

ACKNOWLEDGMENTS

C.P.Y. is grateful to Shi-Biao Zheng for very useful comments. This work is supported in part by the National Natural Science Foundation of China under Grant No. 11074062, the Zhejiang Natural Science Foundation under Grant No. Y6100098, funds from Hangzhou Normal University, and the Open Fund from the SKLPS of ECNU.

-
- [1] Barenco A, Bennett C H, Cleve R, DiVincenzo D P, Margolus N, Shor P, Sleator T, Smolin J A and Weinfurter H 1995 *Phys. Rev. A* **52** 3457
 - [2] Möttönen M, Vartiainen J J, Bergholm V and Salomaa M M 2004 *Phys. Rev. Lett.* **93** 130502
 - [3] Bergholm V, Vartiainen J J, Möttönen M and Salomaa M M 2005 *Phys. Rev. A* **71** 052330
 - [4] Wang X, Sørensen A and Mølmer K 2001 *Phys. Rev. Lett.* **86** 3907
 - [5] Yang C P and Han S 2005 *Phys. Rev. A* **72** 032311
 - [6] Duan L M, Wang B and Kimble H J 2005 *Phys. Rev. A* **72** 032333
 - [7] Lin X M, Zhou Z W, Ye M Y, Xiao Y F and Guo G C 2006 *Phys. Rev. A* **73** 012323
 - [8] Xiao Y F, Zou X B and Guo G C 2007 *Phys. Rev. A* **75** 054303
 - [9] Zou X B, Xiao Y F, Li S B, Yang Y and Guo G C 2007 *Phys. Rev. A* **75** 064301
 - [10] Lin G W, Zou X B, Lin X M and Guo G C 2009 *Phys. Rev. A* **79** 064303
 - [11] Shor P W 1994 in *Proceedings of the 35th Annual Symposium on Foundations of Computer Science* (IEEE Computer Society Press, Santa Fe, NM)

- [12] Grover L K 1997 *Phys. Rev. Lett.* **79** 325
- [13] Shor P W 1995 *Phys. Rev. A* **52** R2493; Steane A M 1996 *Phys. Rev. Lett.* **77** 793
- [14] Zhang J, Liu W, Deng Z, Lu Z and Long G L 2005 *J. Opt. B: Quantum Semiclass. Opt.* **7** 22
- [15] Monz T, Kim K, Hänsel W H, Riebe M, Villar A S, Schindler P, Chwalla M, Hennrich M and Blatt R 2009 *Phys. Rev. Lett.* **102** 040501
- [16] Mottonen M, Vartiainen J J, Bergholm V and Salomaa M M 2004 *Phys. Rev. Lett.* **93** 130502
- [17] Sasura M and Buzek V 2001 *Phys. Rev. A* **64** 012305
- [18] Mottonen M, Vartiainen J J, Bergholm V and Salomaa M M 2005 *Quant. Inf. Comp.* **5** 467
- [19] Laflamme R, Miquel C, Paz J P and Zurek W H 1996 *Phys. Rev. Lett.* **77** 198
- [20] Beth T and Ötteler M R 2001 *Quantum Information* (Springer, Berlin), Vol. **173**, Ch. 4, p. 96
- [21] Bartkiewicz K, Miranowicz A and Ozdemir S K 2009 *Phys. Rev. A* **80** 032306
- [22] Dur W, Vidal G and Cirac J I 2000 *Phys. Rev. A* **62** 062314
- [23] Hofheinz M, Wang H, Ansmann M, Bialczak R C, Lucero E, Neeley M, O'Connell A D, Sank D, Wenner J, Martinis J M and Cleland A N 2009 *Nature* (London) **459** 546
- [24] You J Q and Nori F 2005 *Phys. Today* **58** (11) 42
- [25] Liu Y X, You J Q, Wei L F, Sun C P and Nori F 2005 *Phys. Rev. Lett.* **95** 087001
- [26] Clarke J and Wilhelm F K 2008 *Nature* (London) **453** 1031
- [27] Neeley M, Ansmann M, Bialczak R C, Hofheinz M, Katz N, Lucero E, O'Connell A, Wang H, Cleland A N and Martinis J M 2008 *Nature Physics* **4** 523; Zagoskin A M, Ashhab S, Johansson J R and Nori F 2006 *Phys. Rev. Lett.* **97** 077001
- [28] Makhlin Y, Schön G and Shnirman A 2001 *Rev. Mod. Phys.* **73** 357
- [29] Makhlin Y, Schn G and Shnirman A 1999 *Nature* (London) **398** 305
- [30] Yang C P, Chu Shih-I and Han S 2003 *Phys. Rev. A* **67** 042311
- [31] Yang C P, Liu Y X and Nori F 2010 *Phys. Rev. A* **81** 062323
- [32] Zheng S B and Guo G C 2000 *Phys. Rev. Lett.* **85** 2392
- [33] Zheng S B 2008 *Phys. Rev. A* **77** 033852
- [34] Yu Y and Han S, Private Communication (2011)
- [35] Yang C P, Chu Shih-I and Han S 2004 *Phys. Rev. A* **70** 044303
- [36] DiCarlo L, Reed M D, Sun L, Johnson B R, Chow J M, Gambetta J M, Frunzio L, Girvin S M, Devoret M H and Schoelkopf R J 2010 *arXiv* 1004.4324
- [37] DiCarlo L, Chow J M, Gambetta J M, Bishop L S, Johnson B R, Schuster D I, Majer J, Blais A, Frunzio L, Girvin S M and Schoelkopf R J 2009 *Nature* (London) **460** 240
- [38] Leek P J, Filipp S, Maurer P, Baur M, Bianchetti R, Fink J M, Goppl M, Steffen L and Wallraff A 2009 *Phys. Rev. B* **79** 180511(R)
- [39] Day P K, LeDuc H G, Mazin B A, Vayonakis A and Zmuidzinas J 2003 *Nature* (London) **425** 817